Bioactive sol-gel foams for tissue repair

Pilar Sepulveda,* Julian R. Jones, Larry L. Hench
Centre for Tissue Engineering and Repair, Department of Materials, Imperial College of Science, Technology and Medicine, Prince Consort Road, London SW7 2BP, United Kingdom

Received 5 June 2001; accepted 12 June 2001

Abstract: Bioactive glasses are known to have the ability to regenerate bone, but their use has been restricted mainly to powder, granules, or small monoliths. This work reports on the development of sol-gel foams with potential applications as bone graft implants or as templates for the *in vitro* synthesis of bone tissue for transplantation. These bioactive foams exhibit a hierarchical structure with interconnected macropores (10–500 μm) and a mesoporous framework typical of gel–glasses (pores of 2–50 nm). The macroporous matrixes were produced through a novel route that comprises foaming of sol-gel systems. Three glass systems were tested to verify the applicability of this manufacturing route, namely SiO_2, SiO_2-CaO, and SiO_2-CaO-P_2O_5. This new class of material combines large pores to support vascularization and 3-D tissue growth with the ability that bioactive materials have to provide bone-bonding and controlled release of ionic biologic stimuli to promote bone cell proliferation by gene activation. © 2001 John Wiley & Sons, Inc. J Biomed Mater Res 59: 340–348, 2002

Key words: foam; bioactivity; tissue engineering; bone grafts; porous ceramics

INTRODUCTION

When a significant loss of tissue occurs as a result of trauma or through the excision of diseased or cancerous tissue, healing occurs only with the aid of graft implants. Therapies that employ graft material retrieved from a different site in the patient (autograft), from another human donor (homograft), or from other living or nonliving species (heterografts or xenografts) have been restricted by limited material availability, complicated multistage surgery at the detriment of the harvest site, and the risk of disease transmission.[1] These factors create a great demand for synthetic substitutes especially designed and manufactured to suit the functionality and biocompatibility criteria of tissue engineering.

The tissue restorative potential of bioactive materials long has been demonstrated through both *in vivo* studies and in clinical practice, such as periodontal repair,[2] alveolar bone augmentation,[3] and middle ear devices.[4] Certain compositions of bioactive glasses containing SiO_2-CaO-P_2O_5 bond to both soft and hard tissue without an intervening fibrous layer. Results of *in vivo* implantation show that these compositions produce no local or systemic toxicity, no inflammation, and no foreign-body response.[5–7] The bioactivity has been associated with the formation of a crystalline hydroxyapatite surface layer, similar to the structure of the inorganic region of bone, on contact with body fluid.[7] Recently, Xynos et al.[8–10] have shown that bioactive glass dissolution products exert a genetic control over the osteoblast (bone progenitor cells) cell cycle and the rapid expression of genes that regulate osteogenesis and the production of growth factors. These discoveries have stimulated more extensive investigations of bioactive glass usage as scaffolds for tissue engineering.

It is important to note that in order to repair large defects, 3-D scaffolds are required to provide a template and support tissue growth rather than the usual powder or granular form in which bioactive glasses currently are commercially produced. Ideally the template must consist of (1) an interconnected network with large pores (greater than 100 μm) to enable tissue ingrowth and nutrient delivery to the center of the regenerated tissue;[11] and (2) pores in the microporous (<2 nm) or mesoporous (2 nm < pore size < 50 nm) range to promote cell adhesion, adsorption of biologic metabolites,[12] and resorbability at controlled rates to match that of tissue repair.

*Present address: Instituto de Pesquisas Energéticas e Nucleares, IPEN/CNEN, Divisão de Materiais Cerâmicos, Travessa R, 400 - Cidade Universitária, São Paulo, SP, CEP 05508-900 Brazil

Correspondence to: P. Sepulveda; e-mail: pilarsi@net.ipen.br

Contract grant sponsor: FAPESP, Brazil; contract grant number: 99/02172-4 (postdoctoral grant)

Contract grant sponsor: EPSRC

This manuscript presents a processing route to obtain such a structure. Compositions of sol-gel-derived bioactive glasses were used because they exhibit high specific area, high osteoconductive properties, and also a significant degradability.[13] The art of bioactive foam manufacture was based on previous work by the primary author of porous ceramics production via foaming of colloidal suspensions. In the previous method, foamed suspensions were solidified by the *in situ* polymerization of organic monomers, creating a crosslinked polymeric network (gel) to sustain the foam.[14] The critical step of processing was the control of the onset of gelation, required to prevent drainage of the liquid foam films that would produce poor macro and microstructures. The same principles that pertained for obtaining porous materials are also valid for the foaming of sol-gels, the difference being the setting mechanism, which in the latter is accomplished by fast condensation using catalysts such as acids or bases.

The steps for making these macroporous sol-gel-derived bioactive glasses, termed bioactive foams, and their characterization for physical properties are shown herein. The glasses can be manufactured with specific architectures to obtain controlled rates of glass resorption and rates of chemical dissolution of species that promote tissue regeneration, thus creating a novel three–dimensional tissue construct similar to natural tissues. A range of potential applications is possible for the repair and reconstruction of diseased and damaged tissue, as matrices for graft implant materials, or as devices for the controlled release of biologic or pharmaceutical substances.

MATERIALS AND METHODS

The macroporous scaffolds were prepared by the foaming of sol-gel systems, using a combination of previously established procedures.[14,15] The steps for manufacture are illustrated in Figure 1. In order to verify the process applicability to various systems, the procedure was carried out using three compositions: the pure silica SiO_2 (100S), the binary 70% SiO_2-30% CaO (70S30C), and the ternary 60% SiO_2, 36% CaO, 4% P_2O_5 (58S) systems, in molar percentage. The two latter compositions have been investigated by Professor Hench's team at the Imperial College and have demonstrated high bioactivity *in vitro*[16,17] and *in vivo*.[12] The sol-gel precursors used in this study were tetraethoxyl orthosilicate [TEOS, $Si(OC_2H_5)_4$], triethoxyl orthophosphate [TEP, $OP(OC_2H_5)_3$], and calcium nitrate $Ca(NO_3)_2 \cdot 4H_2O$, hydrolyzed in the presence of 2*N* of nitric acid (HNO_3).

Initially the procedure involved preparing the sol-gel by a mixture of distilled water, the appropriate alkoxide precursors and salts, and the catalyst for hydrolysis, nitric acid. On completion of hydrolysis, aliquots of 50 mL of sol were foamed with the addition of surfactants (polyethylene glycol trimethylnonyl ether, Tergitol TMN10, and Teepol, an ionic surfactant) and vigorous agitation. The concentration of surfactant was varied to obtain specimens with various fractions of porosity. The condensation was catalyzed with an acidic addition (0.1 wt % HF). As the sol viscosity started to rise more steeply, the foamed sols were transferred to molds with the required shape and size, then sealed to age. Sols gelled in the nonfoamed state also were produced for comparison. Aging was carried out at 60°C for 72 h. Slow solvent evaporation then was allowed with the opening of containers and a controlled temperature increase up to 130°C. Thermal stabilization by a heating cycle up to 600°C was carried out to allow partial densification of the matrix.

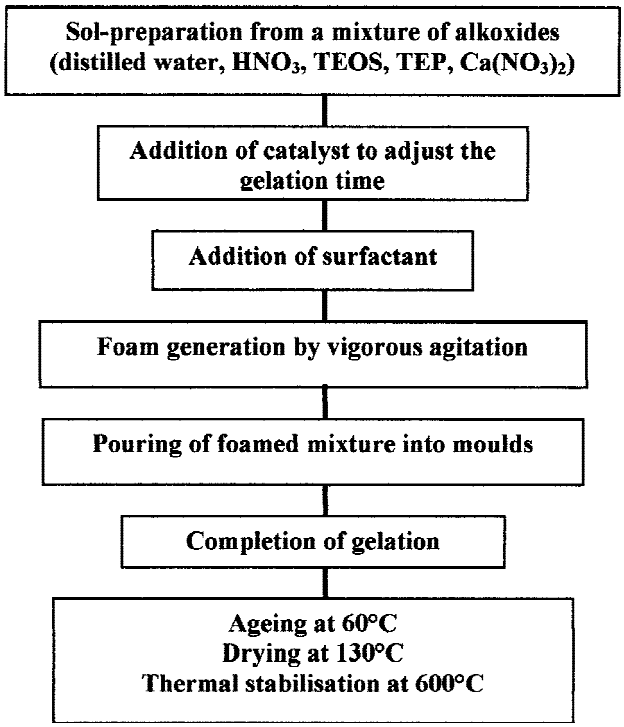

Figure 1. Schematic representation of the manufacture of sol-gel foams.

Physical characterization of the porous foams consisted of microstructural observation, pore size, and textural analysis. Scanning electron microscopy (JEOL, JSM T220A) on gold-coated specimens was used to examine the morphologic and textural features of the foams. Larger pore size ranges were assessed by intrusion mercury porosimetry (PoreMaster 33, Quantachrome).[18] The specific surface area and the porosity in the framework were determined by nitrogen adsorption technique (Autosorb AS6, QuantaChrome). For these experiments, accurately measured weights of small specimens were submitted to evacuation and pretreatment at 100°C for 15 h to remove moisture and contaminants before measurements were made. The volume of nitrogen adsorbed and desorbed at different relative pressures was measured, generating isotherm curves. The first seven points of the adsorption branch (relative pressures of 0.05–0.3) in the isotherms that follow an initial linear trend and imply monolayer formation were fitted to the B.E.T. equation for determination of the specific surface area.[19] The pore diameter distribution was calculated by the BJH method applied to the desorption

curves. Desorption is preferred to adsorption for these calculations because it usually occurs at a lower relative pressure, which is considered to be a better approximation of thermodynamic equilibrium.[19] The types of isotherms were evaluated according to their shape and type of hysteresis between the adsorption–desorption modes.

RESULTS

Flawless foamed glasses successfully can be produced with different compositional systems. A wide range of shapes and sizes was attained with different molds, with no evidence of heterogeneities or phase separation, demonstrating the technique's versatility.

The sol aliquots (50 mL) foamed up to volumes of approximately 1, 2, and 3 times the original volume of sol are identified herein as low, medium, and high foam, respectively. It was difficult to obtain an accurate measure of the final foam volume because it continuously increased until the moment of gelation. Agitation was stopped only at the instant of pouring to avoid collapse of the foam, which occurs spontaneously by liquid drainage.[20]

In spite of the anti-foaming nature of silica solutions,[21] foaming of the sols was accomplished without great complications. A substantial increase in foam volume and foam stability was attained when the sol viscosity started to rise as a result of gelation. The steps of foam generation, pouring into molds, and gelation were completed within 10–15 min. Drying of highly porous specimens occurred without deleterious effects to the structure. Low-foamed specimens required more careful drying as the macroporosity is predominantly closed and solvent evaporation stresses are higher.[22]

Figure 2 shows the macroporous structures of bioactive foams observed by SEM for the three tested compositions, 100S, 70S30C, and 58S. The structures resemble the hierarchy of trabecular bone,[1] forming a template of intricate shape that surrounds large spherical pores. These pores communicate through channels of smaller size. In previous works that reported on the foaming of porous ceramics, it was demonstrated that the degree of foaming has a direct correlation with density, pore size, connectivity of the macroporous structures, and other properties such as permeability and strength of materials with similar structures.[14,23,24] Because of the similarity in structure, these associations are expected to be the same for the foams produced in this work.

Figures 3 and 4 show the mercury porosimetry curves of a few selected specimens of different porosity (70S30C) depending on the produced foam volume and of different compositions at high foam, respectively. Pore-size diameters vary widely from 10 to 200

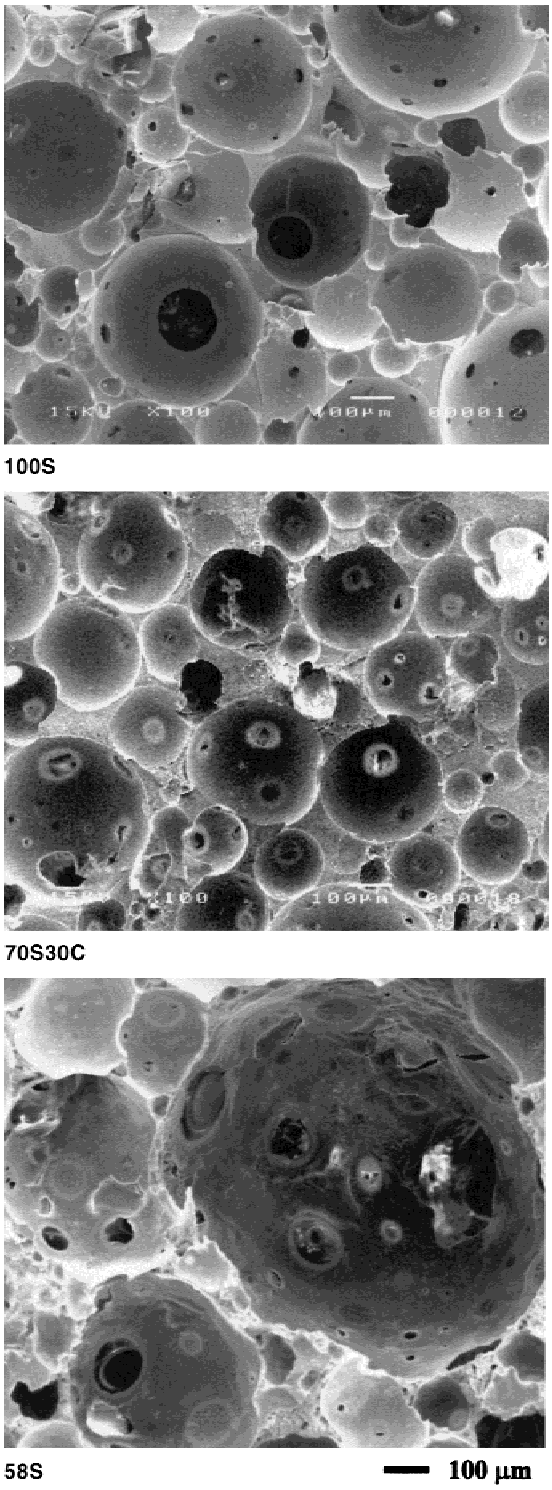

Figure 2. Illustration of structure of 100S, 70S30C, and 58S foams after thermal stabilization at 600°C.-

μm or larger, in ranges determined by the foam volume. More highly foamed sols produce bodies with larger pore size, and nonfoamed specimens have no macroporosity. The measured pore-size values represent the large pores on the specimen surface and the interconnecting windows between pores through

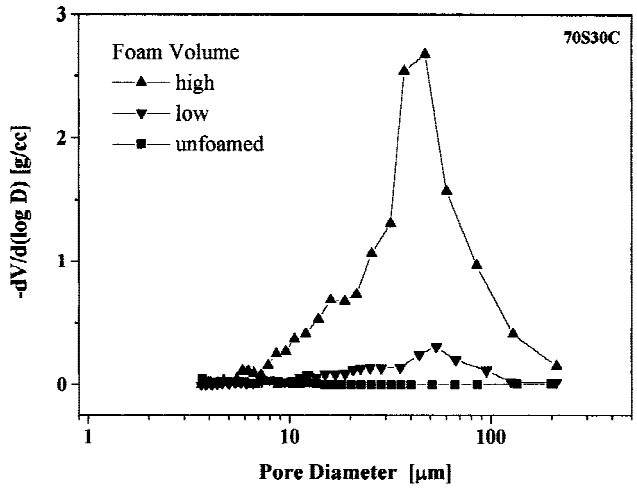

Figure 3. Influence of foam volume on the pore-size distribution measured by mercury porosimetry.

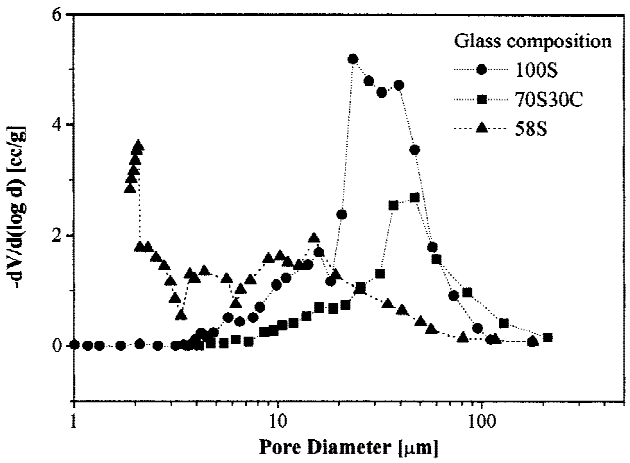

Figure 4. Pore-size distribution of highly foamed 100S, 70S30C, and 58S by mercury porosimetry.

which mercury intrudes the specimen. Although the equipment can measure pores of a maximum size of approximately 300 μm, the structures reveal pore diameters in the range of 500 μm.

The textural features of the solid matrix that forms the template were assessed through a nitrogen sorption technique; the results are given in Table I for various compositions and foam volumes. The surface area of the foamed glasses was very high, in the range of 106–283 m^2/g and generally increased with higher degrees of foaming. The C-constant obtained in multipoint analysis for these materials varied between 65 and 267, giving an indication of the high adsorbate–adsorbent interaction energy.

Figures 5, 6, and 7 show the nitrogen sorption isotherms of bioactive foams at various levels of foaming, and Figures 5, 6, and 7 show the corresponding pore size distributions. All foams yield a type IV isotherm, according to BDDT classification,[19] which is indicative of mesoporous materials (2 to 50 nm). A very steep slope at high relative pressures is associated with capillary condensation in the pores and a narrow pore-size distribution. The hysteresis loops between adsorption and desorption modes are typical for materials with cylindrical pores. The nitrogen sorption results combined with mercury porosimetry results indicate that the bioactive foams are 3-D hierarchical structures of an interconnected macropore network in a matrix containing mesopores. A less steep vertical rise and fall of the isotherms is noted for higher foam volumes. This implies that more highly foamed glasses may combine pores in the mesoporous and macroporous ranges up to approximately 200–300 nm although the average pore size shows a slight variation in the range of 10–30 nm. The matrix of nonfoamed glasses yields a very narrow pore size distribution.

The textural features of the matrix can be confirmed through high magnification SEM, shown in Figures 8, 9, and 10, for 100S, 70S30C, and 58S compositions. Observations show that the texture somehow is affected by the composition and by the foam volume. Pure silica 100S specimens reveal little textural variation (Fig. 8). 70S30C foamed specimens display a slightly more open pore texture than the low-foamed and nonfoamed specimens (Fig. 9). The influence of foam volume on the texture of 58S compositions is

TABLE I
Data of Surface Area, Average Pore Size, and Pore Volume, Measured by Nitrogen Sorption Analysis, of the Foamed Glass Framework at Various Densities

Composition	Degree of Foaming	Surface Area m^2/g	Average Pore Size nm	Pore Volume cc/g
SiO_2	Nonfoamed	114.1	10.13	0.307
	low	267.2	23.78	1.659
	high	282.5	24.76	1.784
70S30C	Nonfoamed	106.8	19.35	0.541
	low	167.3	17.27	0.810
	high	150.8	27.83	1.065
58S	Nonfoamed	146.4	14.25	0.591
	low	239.6	20.13	1.288
	high	233.9	15.21	0.576

more evident, as seen by the pores in the micrometer range that appear on the surface of highly foamed specimens (Fig. 10). These results are confirmed by nitrogen sorption results (Fig. 7), which reveal less steep isotherms without the plateaus at high relative pressures and broader pore size distributions for 58S compositions; however, the differences in pore size and surface area averages are negligible. The mercury porosimetry of highly foamed 58S also shows pores in the micrometer size range, which is different from other systems (Fig. 4). Systems containing more than one component require different thermal stabilizing temperatures to achieve densification and are more prone to phase separation or heterogeneities. A model of aggregation during condensation was suggested by Jokinen and collaborators,[25] who indicated that the change in composition influences the structure, porosity, pore sizes, surface roughness, and surface changes of sol-gel materials. Also, it was shown that the composition affects the reaction kinetics and aggregation mechanisms that determine the pore structure.

The majority of samples produced showed good handling resistance and were significantly strengthened by the use of higher stabilization temperatures, that is, in the range of 600°–800°C.

DISCUSSION

The bioactive sol-gel foams represent a new and promising alternative material for tissue engineering as they combine several valuable properties, as discussed below.

Bioactivity

Bioactive materials typically undergo a rapid rate of surface reaction in contact with body fluids.[5–7] The condensation of a gel layer on the glass surface follows this stage. The biochemical changes caused by glass dissolution and the large amounts of calcium and phosphate ions available in the surrounding tissue stimulate the deposition of an amorphous calcium phosphate layer on the surface of the implant. Further layer deposition and crystallization of the Ca-P-rich layer can occur with absorption of biologic moieties into the structure, binding the inorganic implant to the organic constituents of surrounding tissues.[7] The binary and ternary glass compositions tested in this work were chosen because of their known bioactivity.[15,16] Sol-gel systems such as pure silica and titanium oxide were shown to be bioactive although they lack calcium and phosphate in their compositions.[26,27] The possibility of creating a 3-D framework with these glass compositions provides an important tool for controlling dissolution rates and bioactivity.

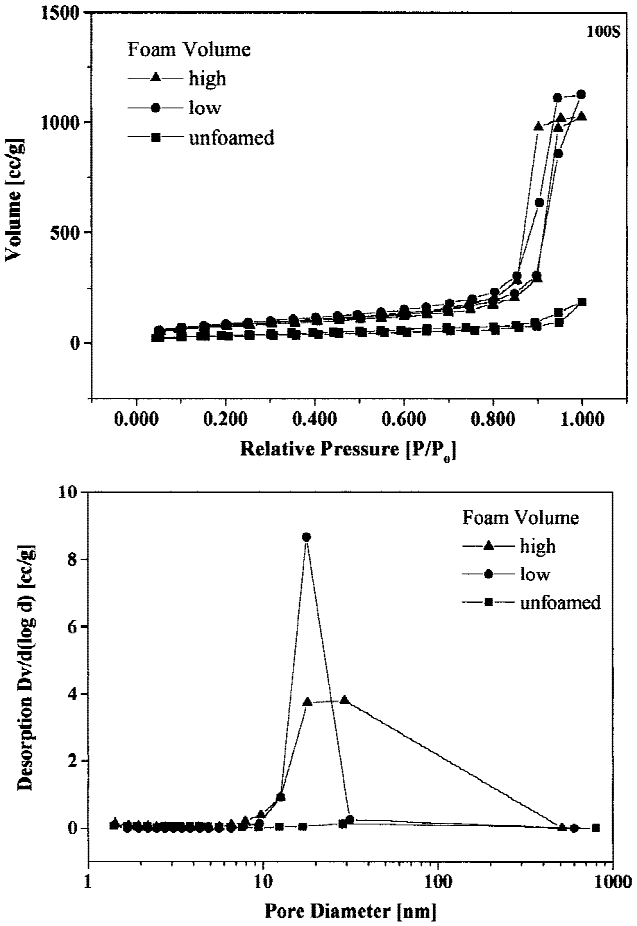

Figure 5. Nitrogen adsorption–desorption isotherms of 100S bioactive foams at various degrees of foaming and the corresponding pore-size distribution.

Sol-gel texture

The mesoporous texture and high surface area of the bioactive foam framework are typical features of sol-gel-derived materials.[28,29] These characteristics intensify the rate of surface reactions, leading to faster release of ionic species during glass dissolution and to a large number of nucleation sites for calcium-phosphate layer deposition compared to dense melt-derived glasses.[30,31] In addition, mesoporosity offers a means of adsorbing and desorbing a range of biologically active substances, such as proteins and growth factors, without loss of conformation and biologic function.[12] The texture of sol-gel materials can be varied through different processing conditions; thus dissolution rates and surface chemical binding sites can be controlled in sol-gel products. This stimulates applications as delivery devices or as devices for eliciting specific *in vitro* culture behaviors.[32]

Macroporous structure

It is well known that a suitable macroporous network is required in tissue engineering scaffolds to en-

able complete access of nutrients to the cells, tissue ingrowth with vascularization, and good integration with host tissues when implanted.[1] Tissue ingrowth rates depend greatly upon pore morphology, the degree of pore connectivity, and pore volume. The open network of large pores of the bioactive foams and the intricate arrangement of the walls are potential features of scaffolds for 3-D tissue repair. The regenerative potential of foamed structures like the ones reported herein was shown previously for hydroxyapatite tested for biocompatibility *in vivo*.[33] HA foams with 85–90% porosity were filled almost entirely with trabecular bone within 8 weeks of implantation in rabbit tibia. The work confirmed the high osteoconductive behavior of HA and the ability of the porous network to promote tissue ingrowth.[33] This behavior is expected improve significantly if the foams are made from class A bioactive compositions.

Resorbability

Depending on the desired application of scaffolds, resorbability may be a necessary property. The resorption rates can be tailored by controlling pore structure and by changing the composition so that they dissolve at controlled rates, matching those of tissue growth. Regenerative bioactive materials resorb at rates that are molecularly controlled by the metabolic processes of the tissues being replaced.[34] A recent work has shown absorbability for bulk sol-gel-derived glasses (58S and 77S Bioglass®) after 12 weeks of implantation, reaching 40% absorption after 52 weeks. No degradation could be measured in the case of 45S5 melt-derived Bioglass®. New bone formation was found to fill in areas that had been resorbed, similar to bone remodeling.[13]

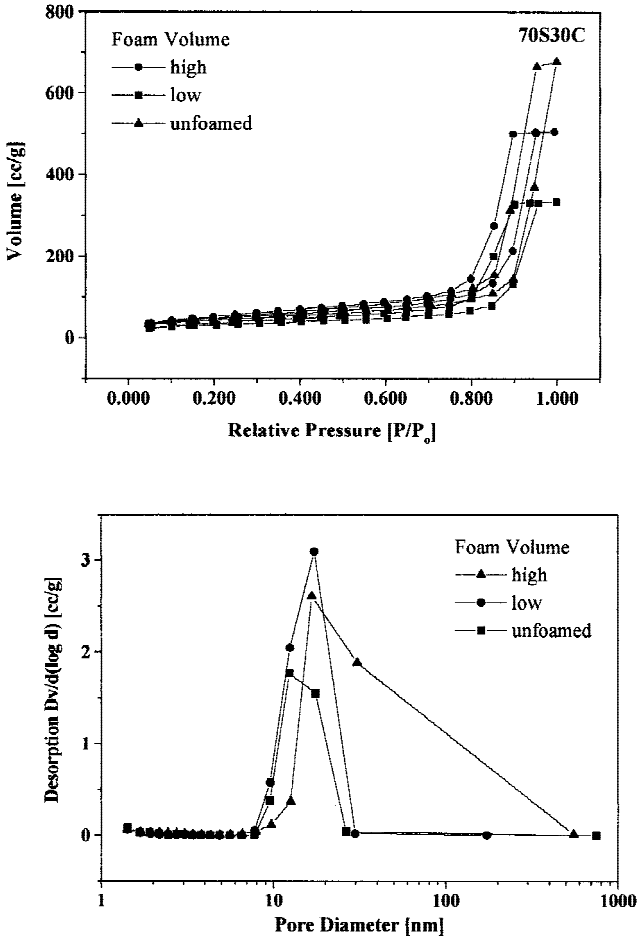

Figure 6. Nitrogen adsorption–desorption isotherms of 70S30C bioactive foams at various degrees of foaming and the corresponding pore-size distribution.

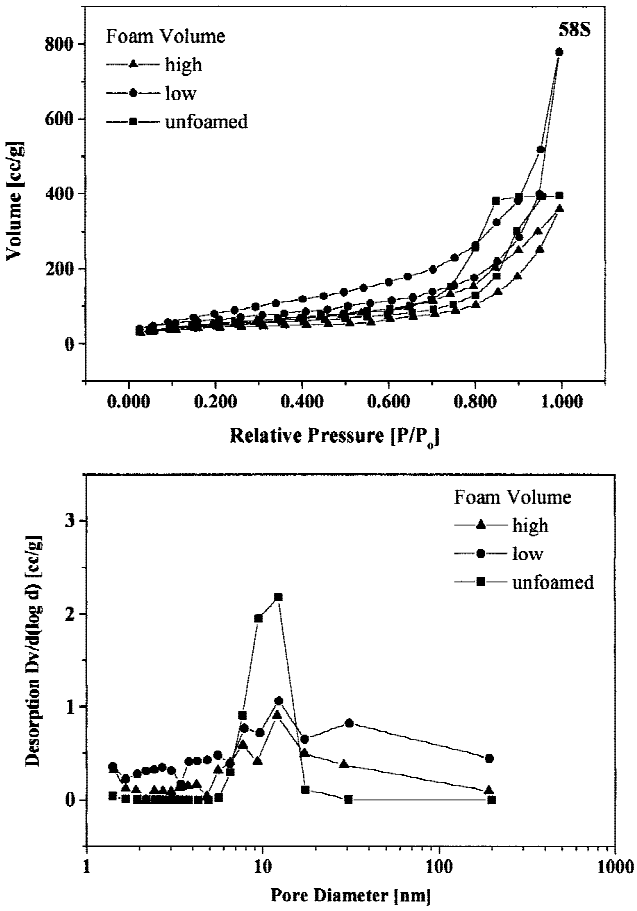

Figure 7. Nitrogen adsorption–desorption isotherms of 58S bioactive foams at various degrees of foaming and the corresponding pore-size distribution.

Genetic stimuli

Mechanisms that may explain the potential of bioactive glasses to regenerate bone tissue were investigated by Xynos et al.[8–10] The experiments were based on *in vitro* cultures of primary human osteoblasts ex-

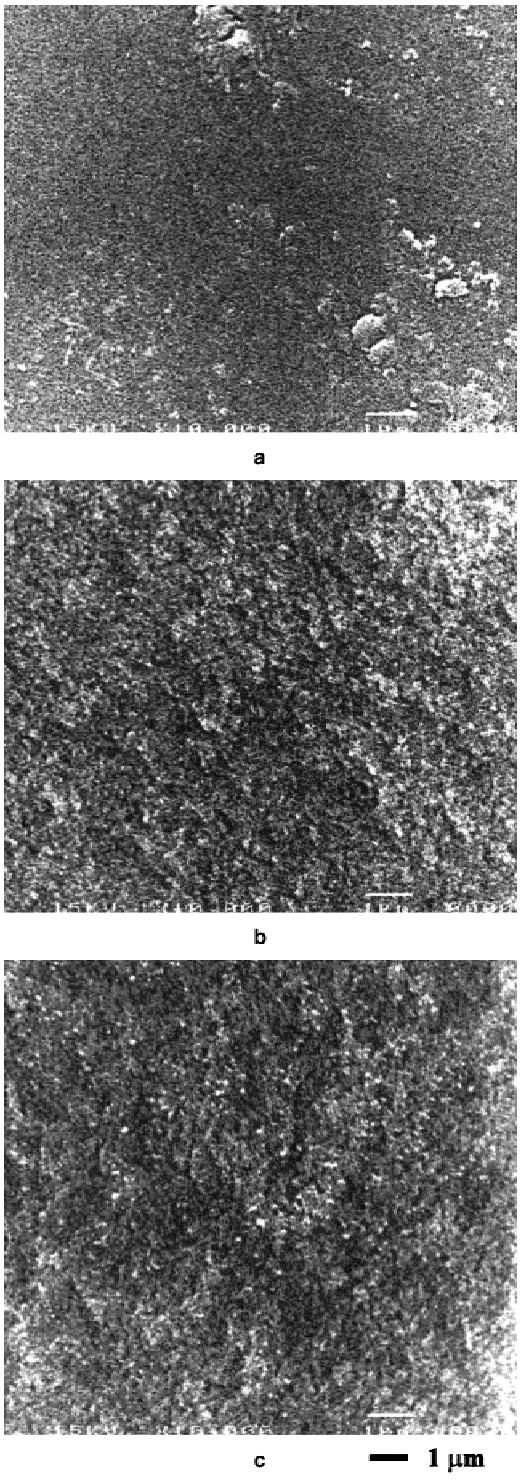

Figure 8. Micrographs of 100S sol-gel, nonfoamed (a), low foam (b), and high foam (c).

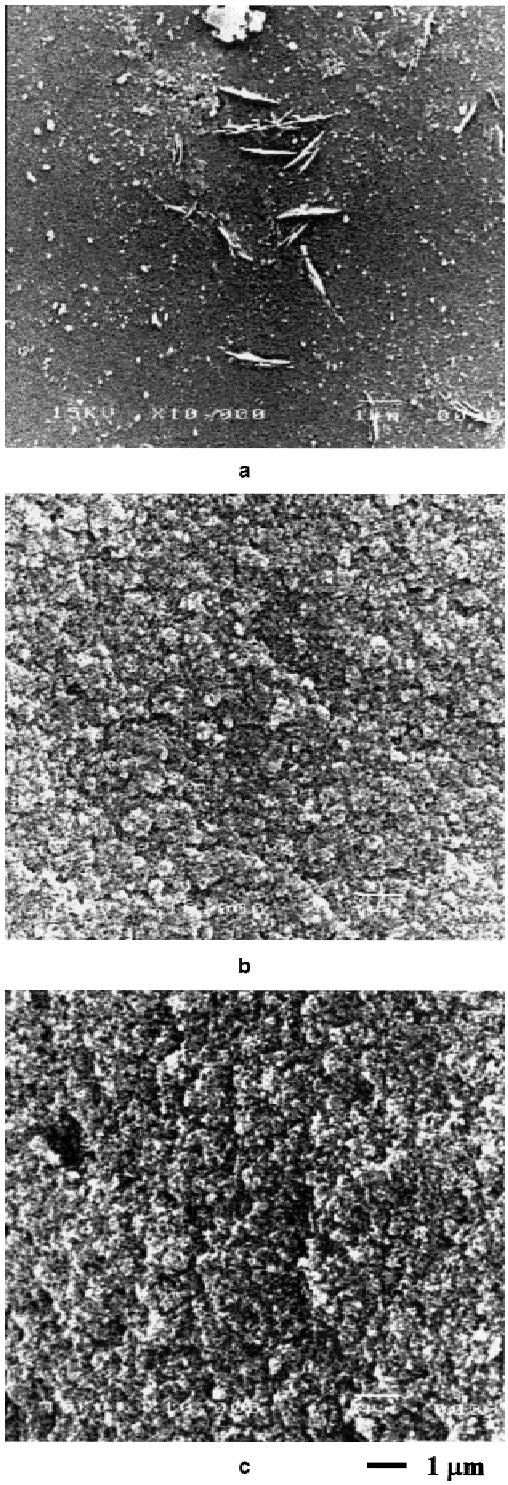

Figure 9. Micrographs of 70S30C sol-gel, nonfoamed (a), low foam (b), and high foam (c).

posed to the extract of 45S5 Bioglass®. Results revealed that the chemical species released from the glasses and their relative concentrations play a specific role in stimulating the activation of genes that control the cell cycle leading to differentiation and proliferation of bone cells.[8] Among the groups of genes that were activated were genes encoding nuclear transcription factors and growth factors such as IGF-II. Mature phenotype osteoblasts and formation of large three-dimensional bone nodules were observed within 6 days *in vitro*. Use of the bioactive foams presented in

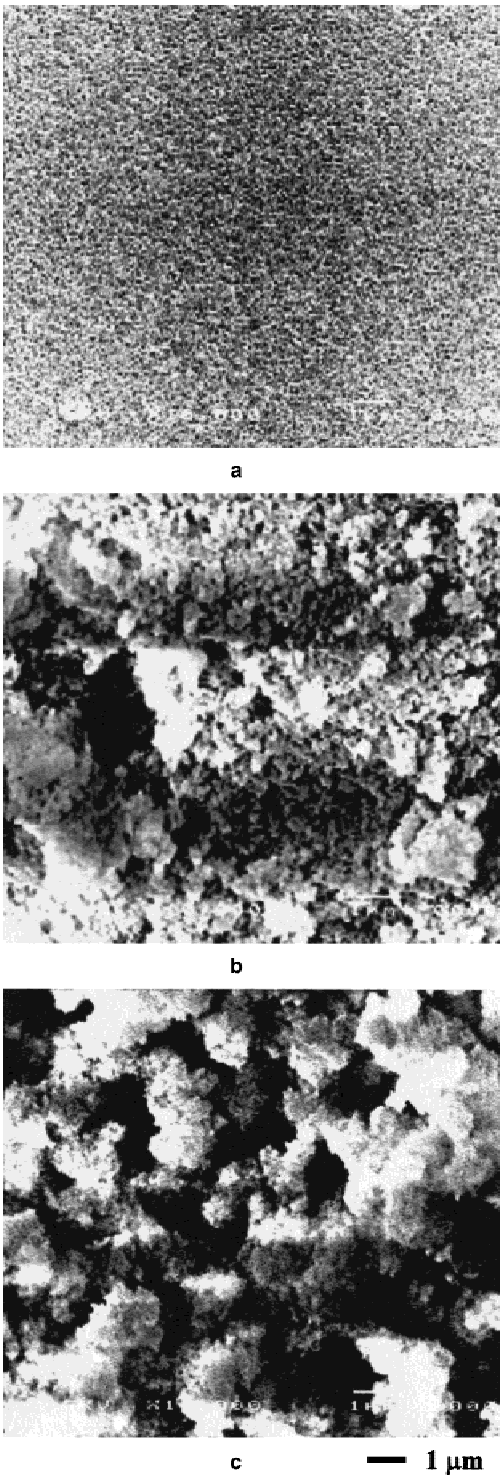

Figure 10. Micrographs of 58S sol-gel, nonfoamed (a), low foam (b), and high foam (c).

this work to direct the growth and organization of bone nodules currently is being investigated.

CONCLUSIONS

Bioactive foams are new materials with the potential of enhancing tissue regeneration. Their macroporosity, matrix texture, and composition can be designed to suit and/or to control the kinetics of interfacial reactions and varied to achieve a tissue's restorative potential. In this work, sol-gel and foaming technologies were combined to create novel materials with applications to the repair and reconstruction of damaged tissue. A hierarchical structure composed of macropores (10–200 μm), mesopores (2–50 nm) and bioactive resorbable compositions potentially can support 3-D organization of cells, enhance cellular differentiation and proliferation, and resorb by controlled rates, thus creating a novel three–dimensional tissue similar to natural tissues and organs. Further studies are in progress to test the *in vitro* dissolution behavior of the bioactive scaffolds and their properties in cell cultures, for future applications as lung tissue repair.

References

1. Ravaglioli A, Krejewski A. Bioceramics: Materials, properties, applications. London: Chapman & Hall; 1992.
2. Zamet JS, Dabar UR. Particulate Bioglass (Perioglass®) in the treatment of periodontal intrabony defects. J Dent Res 76:1997; 291:2219.
3. Norton MR, Wilson J. Bone augmentation with bioactive ceramics before insertion of endosseous dental implants: Histories and human histology on seventeen consecutive cases. Key Eng Mater 2000;192-1:869–872.
4. Wilson J, Clark AE, Douek E, Krieger J, Smith WK, Saville Zamet J. Clinical applications of Bioglass® implants. In: Bioceramics 7. Yli-Urpo OH, Yli-Urpo A, editors. Oxford: Butterworth-Heinemann; 1994. p 415–422.
5. Oonishi H, Hench LL, Wilson J, Sugihara F, Tsuji E, Matsura M, Kin S, Yamamoto T, Mizokawa S. Quantitative comparison of bone growth behavior in granules of bioglass, A-W glass–ceramic, and hydroxyapatite. J Biomed Mater Res 2000;51:37–46.
6. Yamamuro T. A/W glass–ceramics: Clinical applications. In: Hench LL, Wilson J, editors. An introduction to bioceramics. Singapore: World Scientific; 1993. p 89–103.
7. Hench, LL. Bioceramics: From concept to clinic. J Am Ceram Soc 1991;74:1487–1510.
8. Xynos ID, Hukkanen MVJ, Buttery LDK, Hench LL, Polak JM. Bioglass® 45S5 stimulates osteoblast turnover and enhances bone formation in vitro: Implications and applications for bone tissue engineering. Calcif Tissue Int 2000;67:321–329.
9. Xynos ID, Edgar AJ, Buttery LDK, Hench LL, Polak JM. Gene-expression profiling of human osteoblasts following treatment with the ionic products of Bioglass® 45S5 dissolution. J Biomed Mater Res 2001;55:151–157.
10. Xynos ID, Edgar AJ, Buttery LDK, Hench LL, Polak JM. Ionic products of bioactive glass dissolution increase proliferation of human osteoblasts and induce insulin-like growth factor II mRNA expression and protein synthesis. Biochem Biophys Res Comm 2000;276:461–465.
11. Okii N, Nishimura S, Kurisu K, Takeshima Y, Uozumi T. In vivo histological changes occurring in hydroxyapatite cranial reconstruction—Case report. Neurologia Medico-Chirurgica 2001;41:100–104.
12. Hench LL. Sol-gel materials for bioceramic applications. Curr Opin Solid State Mater Sci 1997;2:604–610.
13. Hamadouche M, Meunier A, Greenspan DC, Blanchat C,

Zhong JP, La Torre GP, Sedel L. Absorbability of bulk sol-gel bioactive glasses. Bioceramics 2000;13:593–596.
14. Sepulveda P, Binner JGP. Processing of cellular ceramics by foaming and *in situ* polymerisation of organic monomers. J Eur Ceram Soc 1999:19:2059–2066.
15. Li R, Clark AE, Hench LL. An investigation of bioactive glass powders by sol-gel processing. J Appl Biomater 1991;2:231–239.
16. Saravanapavan P, Hench LL. Low temperature synthesis and bioactivity of gel-derived glasses in the binary CaO-SiO_2 system. J Biomed Mater Res 2001;54:608–618.
17. Cook R, Fielder E, Watson T, Robinson P, Hench LL. Pore characterisation and interconnectivity studies on bioactive 58 S sol-gel glass. Bioceramics 2000;13:625–628.
18. Leon CALY. New perspectives in mercury porosimetry. Adv Colloid Interface Sci 1998;77:341–372.
19. Coleman NJ, Hench LL. A gel-derived mesoporous silica references material for surface analysis by gas sorption. I. Textural features. Ceram Int 2000;26:171–178.
20. Rosen MJ. Foaming and anti-foaming by aqueous solutions of surfactants. In: Surfactants and interfacial phenomena, 2nd ed. New York: Wiley; 1989. p 277–303.
21. Tamura T, Kageyama M, Kaneko Y, Kishino T, Nikaido M. Direct observation of foam film rupture by several types of antifoams using a scanning laser microscope. J Colloid Interface Sci 1999;213:179–186.
22. Hasatani M, Itaya Y. Drying-induced strain and stress: A review. Drying Technol 1996;14:1011–1040.
23. Sepulveda P, Ortega FS, Innocentini MDM, Pandolfelli VC. Properties of highly porous hydroxyapatite obtained by the gel-casting of foams. J Ceram Am Soc 2000;83:3021–3024.
24. Sepulveda P, Binner JGP, Rogero SO, Higa OZ, Bressiani JC. Production of porous hydroxyapatite by the gel-casting of foams and cytotoxic evaluation. J Biomed Mater Res 2000;50: 27–34.
25. Jokinen M, Rahiala H, Rosenholm JB, Peltola T, Kangasniemi I. Relation between aggregation and heterogeneity of obtained structure in sol-gel derived CaO-P_2O_5-SiO_2. J Sol-Gel Sci Technol. 1998;12:159–167.
26. Li PJ, Ohtsuki C, Kokubo T, Nakanishi K, Soga N, De Groot K. The role of hydrated silica, titania, and alumina in inducing apatite on implants. J Biomed Mater Res 1994;28:7–15.
27. Peltola T, Jokinen M, Rahiala H, Levanen E, Rosenholm JB, Kangasniemi I, Yli-Urpo A. Calcium phosphate formation on porous sol-gel-derived SiO_2 and CaO-P_2O_5-SiO_2 substrates *in vitro*. J Biomed Mater Res 1999;44:12–21.
28. Pereira MM, Clark AE, Hench LL. Effect of texture on the rate of hydroxyapatite formation on gel–silica surface. J Am Ceram Soc 1995;78:2463–2468.
29. Pereira MM, Hench LL. Mechanisms of hydroxyapatite formation on porous gel–silica substrates. J Sol-Gel Sci Technol 1996; 7:59–68.
30. Sepulveda P, Jones JR, Hench LL. Characterization of melt-derived 45S5 and sol-gel-derived 58S bioactive glasses. 2001. Submitted for publication.
31. Sepulveda P, Jones JR, Hench LL. *In vitro* dissolution of melt-derived 45S5 and sol-gel-derived 58S bioactive glasses. 2001. Submitted for publication.
32. Bottcher H, Slowik P, Suss W. Sol-gel carrier systems for controlled drug delivery. J Sol-Gel Sci Technol 1998;13:277–281.
33. Sepulveda P, Meseguer L, Bressiani AH, Bressiani JC, König B Jr. *In vivo* properties of foamed HA. 2001. Submitted for publication.
34. Wheeler DL, Eschbach EJ, Hoellrich RG, Montfort MJ, Chamberland DL. Assessment of resorbable bioactive material for grafting of critical-size cancellous defects. J Orthop Res 2000; 18:140–148.